

Convolutional Neural Networks Regularized by Correlated Noise

Shamak Dutta, Bryan Tripp

Systems Design Engineering & Center for Theoretical Neuroscience
University of Waterloo
Waterloo, Canada
{s7dutta,bptripp}@uwaterloo.ca

Graham W. Taylor

School of Engineering, University of Guelph
Vector Institute for Artificial Intelligence
Canadian Institute for Advanced Research
gwtaylor@uoguelph.ca

Abstract—Neurons in the visual cortex are correlated in their variability. The presence of correlation impacts cortical processing because noise cannot be averaged out over many neurons. In an effort to understand the functional purpose of correlated variability, we implement and evaluate correlated noise models in deep convolutional neural networks. Inspired by the cortex, correlation is defined as a function of the distance between neurons and their selectivity. We show how to sample from high-dimensional correlated distributions while keeping the procedure differentiable, so that back-propagation can proceed as usual. The impact of correlated variability is evaluated on the classification of occluded and non-occluded images with and without the presence of other regularization techniques, such as dropout. More work is needed to understand the effects of correlations in various conditions, however in 10/12 of the cases we studied, the best performance on occluded images was obtained from a model with correlated noise.

Index Terms—Correlated Variability, Convolutional Neural Networks, Regularization, Stochastic Neurons

I. INTRODUCTION

Convolutional neural networks (CNN) trained for object recognition tasks are similar to the visual cortex in many ways. For example, early layers show Gabor-like receptive fields similar to V1 [1], late layers that are highly predictive of V4, and inferior temporal cortex (IT) responses [2]. However, these networks lack the correlated variability of neuron responses in the human brain, among other major differences. In this paper, we discuss methods to incorporate correlated variability into deep convolutional networks and analyze its effect on recognition performance.

Studying stochastic neurons is interesting because the effect of stochasticity on learning and computation in artificial neural systems may help us in modeling biological neurons. In population coding schemes in the brain, the joint activities of many neurons encode the value of a quantity. One advantage of population coding is that the noise can be averaged out over many neurons. However, the observation of correlation in spike variability [3] is concerning because it can prevent noise averaging and strongly affect cortical processing. The function of correlated variability in the brain is unclear. Our goal is to understand if correlated variability has benefits that can be realized in artificial neural networks by studying its influence on certain tasks. One example of such a task is the long-standing problem of object recognition under

partial occlusion. This requires the ability to robustly model invariance to certain transformations of the input. The primary method of gaining invariance to transformations is data driven, either by attempting to collect instances of the object under a wide variety of conditions, or augmenting the existing dataset via synthetic transformations. The authors in [4] suggest that the right way to learn invariance is not by adding data, as occlusions follow a long-tail distribution which cannot be covered, even by large-scale efforts in collecting data. This motivates the need to modify the structure of the network to learn invariance. We hypothesize that correlated variability might improve recognition performance in the challenging setting of partial occlusion.

A common approach for regularizing deep neural networks is to inject noise during training; for example, adding or multiplying noise to the hidden units of the neural network, like in dropout [5]. Most solutions include additive or multiplicative independent noise in the hidden units. This is widely used because of its simplicity and effectiveness. We are motivated to consider correlated noise that is dependent on the weights of the network, such as our proposal to add noise sampled from a correlated distribution, where the correlation is a function of the differences in spatial position and selectivity of neurons, similar to the visual cortex. One of the major concerns of stochasticity in neural networks is the tendency to break differentiability, which prevents gradient computation via back-propagation. Depending on the noise distribution, one may simply ignore stochasticity in back-propagation (e.g. the straight-through estimator in the case of binary stochastic neurons [6]), or one may apply computationally convenient estimators for non-differentiable modules. For the latter case, there has been much work focused on back-propagation through non-differentiable functions. For example, the re-parameterization trick in [7] allows for back-propagation through sampling from a broad class of continuous distributions. Re-parameterization using the Gumbel-max trick and the softmax function in [8], [9] allows for back-propagation through samples from categorical discrete distributions. Advancements in the area of back-propagation through non-differentiable modules is relevant to our work because it allows us to consider many interesting types of noise models.

In this paper, we discuss four different types of noise models: independent Gaussian, correlated Gaussian, independent Poisson, and correlated Poisson (Section III-A). In the case of correlation, we also describe how to construct correlation between samples (Section III-B). Finally, we evaluate these different noise models on the classification of occluded and non-occluded images.

II. RELATED WORK

Independent Noise Models: The analysis of noise in deep networks has focused on models that use independent noise to perturb the activations of neurons. For example, dropout [5] is an effective method to regularize neural networks where each unit is independently dropped with a certain probability. Independent Gaussian noise has also been extensively explored in [10], where noise is added to the input, or before or after the non-linearity in other layers. The authors connect different forms of independent noise injection to certain forms of optimization penalties in a special form of a denoising autoencoder. An observation to note is that additive Gaussian noise with zero-mean and variance equal to the unit activation relates to a penalty that encourages sparsity on the hidden unit activations. This is interesting because the time intervals between spikes in a cortical neuron are irregular and can be modeled using a Poisson process, such that the variance of the spike count in a small time interval is equal to the mean spike count. This motivates us to investigate whether we can model artificial neurons as samples from a Poisson distribution. The work done in [10] focused on unsupervised learning in autoencoders and used the learned hidden representations as inputs to a classifier. Our approach differs in the fact that we are directly using a supervised classifier (CNN) to analyze the injection of noise.

Back-propagation Through Random Nodes: Gradient-based learning which leverages back-propagation in neural networks requires that all operations that depend on the trainable parameters be differentiable. Stochastic neural networks usually involve samples from a distribution on the forward pass. However, the difficulty is that we cannot back-propagate through the sampling operation. It is shown in [6] that in the case of injection of additive or multiplicative noise in a computational graph, gradients can be computed as usual. We use this method in Section III-A1. Bengio et al. [6] also introduce the concept of a straight-through estimator, where a copy of the gradient with respect to the stochastic output is used directly as an estimator of the gradient with respect to the sigmoid (or any non-linearity) operator. Similar to the straight-through estimator, in Sections III-A3 and III-A4, we use the expected value of the Poisson distribution as if it were the output of the neuron during back-propagation. The work in [8], [9] allows for back-propagation through samples from discrete categorical distributions. While we do not use this technique in our work, it is possible to choose an upper bound K to convert a Poisson distribution to a categorical distribution of size K . The sample from the distribution would be the expected value

of this estimated categorical distribution and back-propagation can proceed since the entire process is made differentiable.

Augmentation in Feature Space: Dataset augmentation is a cheap and effective way to generate more training data with variability that is expected at inference time. Recently, some works have considered augmentation techniques, such as the addition of noise, as well as interpolation and extrapolation from pairs of examples, not in input space, but in a learned feature space [11], [12]. However, [11] shows that simple noise models (e.g. Gaussian) do not work effectively when compared to extrapolation. We are motivated by the fact that more sophisticated noise models (e.g. correlated) could be useful for feature space-based augmentation.

III. METHODS

A. Noise Framework

We analyzed different types of independent and correlated noise to elucidate their effects on neural networks. This helped us understand the impact of injecting correlated noise when compared to the common practice of injecting independent noise.

1) *Independent Gaussian Noise:* We consider h_i to be the output of a stochastic neuron. The output is a deterministic function of a differentiable transformation a_i and a noise source z_i , as considered in [6]. a_i is typically a transformation of its inputs (vector output of other neurons) and trainable parameters (weights and biases of a network). The output of the stochastic neuron is:

$$h_i = f(a_i, z_i). \quad (1)$$

As long as h_i is differentiable with respect to a_i and has a non-zero gradient, we can train the network with back-propagation. In this section, one form of noise we consider is additive independent Gaussian noise with zero mean and σ^2 variance, where:

$$f(a_i, z_i) = a_i + z_i, \quad (2)$$

$$z_i \sim \mathcal{N}(0, \sigma^2). \quad (3)$$

At test time, we can compute the expectation of the noisy activations by sampling from the distribution $\mathcal{N}(a_i, \sigma^2)$; however, this can be computationally expensive for large datasets. Instead, we can approximate the expectation by scaling the units by their expectation, as in dropout [5]. Since we are using zero mean additive noise, no scaling is required, as the expectation does not change.

A special case of Equation 3 is when $\sigma^2 = a_i$. The distribution of activations for a specific stimulus will follow $\mathcal{N}(a_i, a_i)$, which has a Fano factor of 1. This is similar to biological neurons, which exhibit Poisson-like statistics with a Fano factor of approximately 1. It also means that z_i is now a function of a_i and the gradient of z_i with respect to a_i exists through re-parameterization. A sample from a normal distribution $\mathcal{N}(\mu, \sigma^2)$ can be constructed as:

$$\begin{aligned} x_i &\sim \mathcal{N}(0, 1), \\ z_i &= \mu + \sigma x_i. \end{aligned} \quad (4)$$

In the case when $\sigma^2 = a_i$ and $\mu = 0$, $z_i = \sqrt{a_i}x_i$. In practice, the gradients can be unstable for the square-root function for small values. To solve this problem, we add a small value of $\epsilon = 0.0001$ to the argument of the square-root function.

2) *Correlated Gaussian Noise*: We consider $\mathbf{h} \in \mathbb{R}^n$ to be a vector of outputs of n stochastic neurons. \mathbf{h} is a sum of a noise vector $\mathbf{z} \in \mathbb{R}^n$ and a vector output $\mathbf{a} \in \mathbb{R}^n$, which is a differentiable transformation of its inputs and trainable parameters, similar to Section III-A1. The vector output is:

$$\mathbf{h} = \mathbf{z} + \mathbf{a}, \quad (5)$$

$$\mathbf{z} \sim \mathcal{N}(\mathbf{0}, \Sigma). \quad (6)$$

Given a desired mean $\boldsymbol{\mu}$ and correlation matrix Σ , $\mathbf{z} \in \mathbb{R}^n$ is sampled as follows:

- Sample $\mathbf{X} \sim \mathcal{N}(\mathbf{0}, \mathbf{I}_n)$
- Compute the Cholesky decomposition: $\Sigma = LL^*$, where L^* is the conjugate transpose of L .
- $\mathbf{z} = \boldsymbol{\mu} + L\mathbf{X}$
- If $\boldsymbol{\sigma} \in \mathbb{R}^n$ is the desired standard deviation, then

$$\mathbf{z} = \text{diag}(\boldsymbol{\sigma})(\boldsymbol{\mu} + L\mathbf{X}), \quad (7)$$

where $\text{diag}(\boldsymbol{\sigma}) \in \mathbb{R}^{n \times n}$ is a matrix with the standard deviations on the diagonal and zeros elsewhere.

As described in Section III-B2, the correlation matrix Σ is a function of the trainable weights of the network. This implies that the entire sampling process is differentiable with respect to the parameters μ , σ , and the trainable weights, and that gradient-based learning can proceed as usual.

3) *Independent Poisson Noise*: We consider h_i to be the output of a stochastic neuron. The definition of a_i is the same as in Section III-A1. In the case of independent Poisson noise, the output of the neuron is:

$$h_i \sim \text{Poisson}(\lambda = a_i), \quad (8)$$

where the mean is given by a_i . This poses a problem in back-propagation, as there is no gradient of h_i with respect to the parameter $\lambda = a_i$. The re-parameterization trick in [7] cannot be applied in this case because the Poisson distribution is discrete. To avoid this problem, we set the output of the unit to its mean value during the backward pass, which is a_i . We still propagate the sample from the distribution on the forward pass. This is similar to the straight-through estimator for back-propagation through stochastic binary neurons [6]. The Gumbel-softmax method [8], [9] can be used here if the Poisson distribution is converted to a categorical distribution using an upper threshold K . We plan to explore this avenue in future work.

4) *Correlated Poisson Noise*: Similar to Section III-A2, $\mathbf{h} \in \mathbb{R}^n$ is a vector of outputs of n stochastic neurons. \mathbf{h} is a sample from a correlated Poisson distribution of mean $\boldsymbol{\lambda}$ and correlation matrix Σ ,

$$\mathbf{h} \sim \text{Poisson}(\boldsymbol{\lambda}, \Sigma). \quad (9)$$

We draw approximate samples from this distribution in the following way. Given a desired mean $\boldsymbol{\lambda} \in \mathbb{R}^n$ and correlation matrix $\Sigma \in \mathbb{R}^{n \times n}$:

- Sample $\mathbf{X} \sim \mathcal{N}(\boldsymbol{\mu}, \Sigma)$, where $\boldsymbol{\mu}$ is chosen arbitrarily
- Apply the univariate normal cumulative distribution function (CDF): $\mathbf{Y} = F_x(\mathbf{X}; \mu = 0, \sigma = 1)$
- Apply the quantile (inverse CDF) of the Poisson distribution: $\mathbf{z} \sim F_z^{-1}(\mathbf{Y}; \boldsymbol{\lambda})$

This sampling procedure is non-differentiable for a correlated Poisson. As in Section III-A3, we estimate the gradient using the mean $\boldsymbol{\lambda}$ on the backward pass. The actual correlations between Poisson variables depend on the rates $\boldsymbol{\lambda}$ and are smaller than the desired correlation matrix Σ .

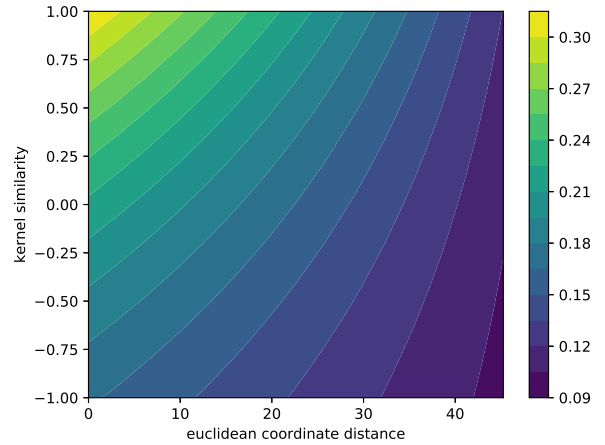


Fig. 1. Correlation dependence on distance and tuning similarity for $a = 0.225$, $b = 0.0043$, $c = 0.09$ and $\tau = 1.87$. The correlation value of the color plot is indicated by the bar on the right.

B. Correlation Matrix

In this section, we discuss how the correlation matrix Σ is constructed, which is used in Sections III-A2 and III-A4. Note that the neuron equivalent in a CNN is a unit in the output feature map of a given layer.

Neurons in the cortex are correlated in their stochasticity. This correlation is a function of the spatial spread and tuning similarity [13]. In the visual cortex, correlations have been studied between neurons in the same visual area. Analogously, we consider correlations between units in the same layer of a CNN. The details of spatial similarity and tuning similarity are described in Sections III-B1 and III-B2. For a given layer in a convolutional network, if the width and height of the feature maps, as well as the number of feature maps are defined as w , h , and k , respectively, then the dimension d of the

correlated distribution we draw samples from is $d = whk$ and the correlation matrix is $\Sigma \in \mathbb{R}^{whk \times whk}$.

Similar to a relationship suggested in [13], the correlation between two neurons, x_1 and x_2 , is determined as:

$$f(x_1, x_2) = [a - b(d(x_1, x_2))]^+ \cdot e^{\frac{k(x_1, x_2) - 1}{\tau}} + c, \quad (10)$$

where $[\cdot]^+$ is $\max(\cdot, 0)$, $d(\cdot, \cdot)$ is a function that returns the scaled Euclidean distance between two neurons, $k(\cdot, \cdot)$ is a function that returns the tuning similarity between two neurons (bounded in $[-1, 1]$), and a , b , c , and τ are hyper-parameters. The correlation is summarized in Figure 1 for specific values of a , b , c , and τ . To summarize, within a layer of a CNN, every neuron is correlated to every other neuron in the same layer by a value determined by how far apart they are and their tuning similarity.

1) *Spatial Similarity*: The spatial similarity between two units in any output feature map within a layer is determined by the Euclidean distance between the coordinates of the neurons within their respective feature maps. The spatial distance between two neurons that are a part of the i^{th} and j^{th} feature maps, respectively, with coordinates $\mathbf{p} = (x_i, y_i)$ and $\mathbf{q} = (x_j, y_j)$ is:

$$d(\mathbf{p}, \mathbf{q}) = \sqrt{(x_i - x_j)^2 + (y_i - y_j)^2}, \quad (11)$$

Since the dimensions of the feature map do not change as training progresses, we can pre-compute the spatial correlations for all pairs of neurons before training begins.

2) *Tuning Similarity*: The tuning similarity between two units in any output feature maps within a layer is determined by the cosine similarity of the normalized weight matrices that produced them. Consider a weight tensor (kernel in a convolutional network) of dimension $d = k \times k \times m \times n$, where k is the kernel size, m is the number of input channels from the previous layer, and n is the number of kernels. The i^{th} kernel \mathbf{w}_i is of dimension $d = kkm \times 1$. The tuning similarity between two neurons in the i^{th} and j^{th} feature maps is determined as:

TABLE I
MODIFIED VERSION OF ALLCONVNET (ALL-CNN-C) ARCHITECTURE WITH 10 FILTERS IN LAYER 1 USED WITH CIFAR-10.

Input: 32×32 RGB image
Layer 1: 3×3 conv. 10 filters, ReLU
Layer 2: 3×3 conv. 96 filters, ReLU
Layer 3: 3×3 conv. 96 filters, stride = 2, ReLU
Layer 4: 3×3 conv. 192 filters, ReLU
Layer 5: 3×3 conv. 192 filters, ReLU
Layer 6: 3×3 conv. 192 filters, stride = 2, ReLU
Layer 7: 3×3 conv. 192 filters, ReLU
Layer 8: 1×1 conv. 192 filters, ReLU
Layer 9: 1×1 conv. 10 filters, ReLU
Layer 10: global averaging over 6×6 spatial dimensions 10-way softmax

TABLE II
STOCHASTIC MODELS EVALUATED AS PART OF LAYER 1 TESTS.

Model name	abbreviation
AllConvNet baseline	Baseline
AllConvNet ind. Gaussian $\sigma = 1.0$	IG_A
AllConvNet ind. Gaussian $\sigma = a_i$	IG_B
AllConvNet correlated Gaussian	CG
AllConvNet ind. Poisson	IP
AllConvNet correlated Poisson	CP

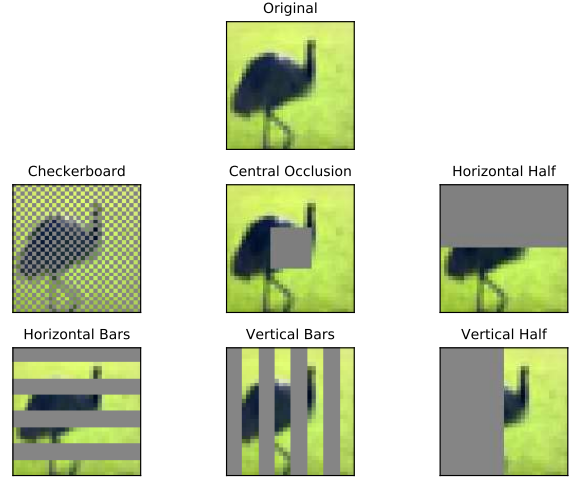


Fig. 2. Different types of occlusions used to evaluate recognition performance. Images shown are taken from CIFAR-10.

$$k(x_i, x_j) = \left(\frac{\mathbf{w}_i}{\|\mathbf{w}_i\|} \right)^T \cdot \frac{\mathbf{w}_j}{\|\mathbf{w}_j\|}, \quad (12)$$

since we are calculating the cosine similarity, $k(\cdot, \cdot) \in [-1, 1]$. Note that the tuning similarity solely depends on the feature maps that the output units are a part of.

IV. EXPERIMENTS

We performed preliminary experiments with the aforementioned noise models using an architecture equivalent to the AllConvnet network [14] (All-CNN-C) with one exception: the first layer contains 10 feature maps instead of 96, as shown in Table I. This was done for computational tractability, as the correlation matrix grows as $(whk)^2$, where w and h are the width and height of a feature map, and k is the number of feature maps in a layer. As a result, the sampling procedure from a correlated distribution can slow training by a large amount. While we do not aim for state-of-the-art results, our goal is to obtain a model that achieves respectable performance on CIFAR-10 and analyze the effect of adding various kinds of noise. All models are trained for 100 epochs and the final chosen model in each case is the one with the lowest validation loss during training to prevent overfitting.

The CIFAR-10 dataset is used for all experiments, split into 50,000 training images and 10,000 test images. The training set does not contain any occluded images. All experiments

TABLE III
 RECOGNITION PERFORMANCE OF LAYER 1 STOCHASTIC BEHAVIOURAL MODELS WITH NO ADDITIONAL REGULARIZATION OVER 10 RUNS

Model	Test Set		Central Occlusion		Checker Board		Horizontal Bars		Vertical Bars		Horizontal Half		Vertical Half	
	mean (%)	s.d. (%)	mean (%)	s.d. (%)	mean (%)	s.d. (%)	mean (%)	s.d. (%)	mean (%)	s.d. (%)	mean (%)	s.d. (%)	mean (%)	s.d. (%)
Baseline	75.5	0.2	62.1	0.1	46.8	0.3	35.7	0.3	34.8	0.4	41.1	0.4	40.3	0.3
IG_A	72.6	0.3	61.6	0.2	45.5	0.2	36.1	0.3	33.0	0.2	43.0	0.3	39.5	0.3
IG_B	75.9	0.1	63.3	0.1	49.6	0.2	41.3	0.4	35.1	0.4	40.6	0.6	37.2	0.3
CG	80.8	0.1	69.1	0.1	58.1	0.2	51.5	0.4	40.6	0.1	47.4	0.3	41.6	0.3
IP	71.8	0.8	59.6	0.5	44.6	0.6	35.2	0.7	32.7	0.4	40.2	0.4	36.3	0.4
CP	76.8	0.5	64.3	0.2	47.5	0.3	44.7	0.3	37.6	0.2	44.6	0.4	45.5	0.2

TABLE IV
 RECOGNITION PERFORMANCE OF LAYER 1 STOCHASTIC BEHAVIOURAL MODELS WITH DROPOUT OVER 10 RUNS.

Model	Test Set		Central Occlusion		Checker Board		Horizontal Bars		Vertical Bars		Horizontal Half		Vertical Half	
	mean (%)	s.d. (%)	mean (%)	s.d. (%)	mean (%)	s.d. (%)	mean (%)	s.d. (%)	mean (%)	s.d. (%)	mean (%)	s.d. (%)	mean (%)	s.d. (%)
Baseline	84.2	0.1	73.8	0.1	63.1	0.1	46.9	0.2	55.1	0.2	47.5	0.2	43.3	0.3
IG_A	85.1	0.1	74.7	0.1	67.3	0.1	50.2	0.3	55.4	0.2	50.6	0.2	46.1	0.3
IG_B	84.5	0.1	74.6	0.1	66.9	0.1	50.1	0.3	56.4	0.2	49.7	0.2	45.8	0.2
CG	84.2	0.1	75.5	0.1	58.4	0.2	54.1	0.2	57.5	0.2	47.4	0.2	47.2	0.2
IP	84.4	0.2	75.1	0.1	63.8	0.1	52.3	0.2	58.2	0.1	49.9	0.2	43.2	0.2
CP	84.9	0.2	75.4	0.1	68.1	0.3	53.1	0.3	57.0	0.1	47.9	0.2	44.6	0.3

were performed using the TensorFlow framework [15]. We evaluate classification performance on the test set, including occluded versions of the test set, as shown in Figure 2.

We first experiment by incremental addition of the stochastic behaviour to understand its effect. The baseline model is described in Table I. First, we add noise in layer 1 of the AllConvNet architecture. The different noise architectures for layer 1 are shown in Table II. The results of this experiment are shown in Section IV-A.

We then analyze whether the benefits of noise can be realized in the presence of another regularizer by evaluating the effect of noise in the presence of dropout. In this case, the baseline model shown in Table I is trained with dropout in specific layers. As before, we add different types of noise to layer 1 in order to understand its impact, as described in Section IV-B.

A. Absence of Dropout

The classification performance of the models that do not incorporate dropout are summarized in Table III. The models are abbreviated, as shown in Table II.

Independent Gaussian noise does not seem to have an appreciable effect on the learning of the network. We varied σ in the set $\{0.1, 0.5, 1.0, 1.5, 2.0\}$ to find the network with the optimal variance, which was $\sigma = 1.0$. It is possible that only adding independent Gaussian noise to one layer is not enough to regularize the network. This motivates the need to add it to multiple layers in order to understand its true effect.

Correlated Gaussian noise achieves the best results at classification of the clean test set, and on five out of the six occlusion classes. The improvement from the baseline model is $\sim 5\%$ after being added only in the first layer, which is encouraging. To ensure that the classification improvement was consistent

across all classes and not only for some outliers, we ran the breakdown of the class predictions for each set shown in Table V. It can be seen that the improvements are consistent for $\sim 70\%$ of different output classes.

Independent Poisson noise has worse performance than the baseline model across all sets. To investigate why this occurred, we examined the distribution of the activations of layer 1 (samples from the Poisson distribution). The values were highly variable in the range $[3, 35]$. This may stem from the fact that we back-propagate the mean rate of the Poisson instead of the actual sample value, which could affect learning. We hypothesize that a penalty on the activations, combined with the independent Poisson noise could achieve acceptable classification results.

The correlated Poisson model also achieves better results than the baseline model across the test set and all occlusion classes and has the best result on the vertical half occlusion set. It also performs better compared to the independent Poisson model across all occlusion sets showing that correlations have an appreciable effect on the classification performance.

B. Presence of Dropout

Dropout was applied to the input image, as well as after each of the layers that has a stride of 2 (simply a convolutional layer that replaces pooling [14], specifically layer 3 and 6). The dropout probability at the input was 20% and was 50% otherwise.

The classification performance of the models that incorporate dropout are summarized in Table IV, with the model abbreviations shown in Table II.

We observe that, when compared to the model without dropout, the baseline model with dropout performed better

TABLE V
CLASS PREDICTION ACCURACY FOR (A) ALLCONVNET BASELINE MODEL WITHOUT DROPOUT AND (B) ALLCONVNET CORRELATED GAUSSIAN MODEL WITHOUT DROPOUT.

Class	Test Set		Central Occlusion		Checker Board		Horizontal Bars		Vertical Bars		Horizontal Half		Vertical Half	
	A	B	A	B	A	B	A	B	A	B	A	B	A	B
airplane	78.9	78.2	73.3	66.6	54.0	52.8	76.9	56.1	51.5	59.3	70.1	70.8	50.1	65.8
automobile	87.7	89.0	79.6	83.1	18.1	29.7	42.1	39.0	18.4	18.5	62.8	63.4	36.2	33.1
bird	69.4	73.2	57.7	58.7	46.2	51.9	32.1	38.2	52.8	57.1	30.5	35.8	79.5	76.0
cat	59.6	62.5	35.2	48.7	37.8	44.2	52.2	44.6	54.8	45.7	19.2	38.0	22.6	42.3
deer	79.6	82.2	68.8	63.4	63.9	69.7	63.1	73.6	50.4	50.7	59.7	58.8	44.1	31.8
dog	70.5	76.1	60.4	72.6	48.4	58.0	32.5	66.7	48.3	68.3	36.7	20.8	38.9	48.5
frog	85.9	88.2	74.5	75.7	64.0	71.4	15.0	42.1	16.9	23.1	60.2	67.0	45.2	32.3
horse	79.2	83.5	71.1	75.1	40.3	51.4	16.9	36.9	37.8	44.3	38.5	41.2	23.5	55.4
ship	88.6	87.8	71.9	73.1	70.0	70.4	51.2	73.6	53.8	47.1	84.8	81.8	73.8	53.1
truck	87.1	89.7	70.5	76.4	67.9	60.7	33.3	26.2	31.2	35.2	41.4	53.0	31.4	47.1

TABLE VI
CLASS PREDICTION ACCURACY FOR (A) ALLCONVNET BASELINE MODEL WITH DROPOUT AND (B) ALLCONVNET CORRELATED POISSON MODEL WITH DROPOUT.

Class	Test Set		Central Occlusion		Checker Board		Horizontal Bars		Vertical Bars		Horizontal Half		Vertical Half	
	A	B	A	B	A	B	A	B	A	B	A	B	A	B
airplane	91.2	86.6	87.2	82.0	81.7	75.4	85.1	71.3	85.7	78.3	89.4	69.3	79.8	76.4
automobile	92.5	93.1	80.6	82.9	38.0	49.5	9.5	20.3	13.8	36.7	56.3	62.8	19.8	34.2
bird	81.7	84.5	65.8	77.1	56.3	69.8	8.3	52.6	44.8	67.8	29.1	54.5	77.0	76.7
cat	75.3	65.8	63.1	53.8	55.6	45.2	10.7	47.4	49.9	49.1	24.3	30.5	50.9	62.5
deer	87.3	83.8	75.4	75.6	80.7	78.9	51.3	83.7	33.3	63.5	64.7	58.8	27.1	59.2
dog	75.7	83.2	57.1	71.9	48.7	62.6	10.9	52.0	54.2	65.7	37.7	40.2	19.7	43.8
frog	92.3	87.5	77.1	69.5	85.5	73.8	0.9	7.2	5.2	36.6	57.1	67.7	17.4	38.5
horse	92.2	91.5	86.5	86.6	61.2	68.2	24.5	55.0	58.1	64.6	54.2	55.2	24.5	46.7
ship	93.0	92.0	82.4	79.9	79.4	82.8	58.6	73.4	67.1	62.7	75.1	88.0	78.5	64.9
truck	90.9	90.3	86.3	85.5	63.9	74.4	18.6	43.5	30.0	58.3	58.9	63.3	10.3	50.4

across all classes with a mean performance increase on the test set of $\sim 10\%$.

Independent Gaussian models improve performance over the baseline model in all sets of images. This is expected, as independent noise is similar to dropout. Hence, it can be interpreted as adding dropout to the first layer of the network, which can explain the performance benefit.

The correlated Gaussian models improved the performance of the network for five out of the seven categories against the baseline model with dropout. This is promising because the addition of dropout into the model with correlated noise increases performance on average.

The independent Poisson model with dropout improved performance against the baseline model with dropout on the test set and six out of the seven occlusion sets. We hypothesized earlier that an activity penalty with an independent Poisson model can lead to strong classification performance, but it seems that dropout along with Poisson noise seems to be a good regularizer for the network.

The correlated Poisson models perform better than the baseline model on all the occluded image sets. The improvements with the correlated model are consistent across different image classes as shown in Table VI.

In general, the addition of correlated noise into the baseline model with and without dropout increases recognition performance across the occlusion sets.

V. CONCLUSION

In this work, we proposed a model of a stochastic neural network whose activity values are correlated based on the spatial spread and selectivity of the neurons. We tested different noise models, as described in Section III-A, on the classification task of occluded and non-occluded images.

A simple model of correlated variability, inspired by the visual cortex, is modeled using the spatial distance between units in an output feature map and the kernel weights that produced them. The variability can be drawn from different distributions of specified correlation; for example, Gaussian and Poisson distributions. Depending on whether the sampling function is differentiable, back-propagation can continue as normal, or it will rely on an estimate of the gradient. There are different methods to estimate the gradient, including re-parameterization and straight-through estimation.

Preliminary results show that correlated variability added to a single layer can perform better than other noise models. In fact, in ten of the twelve occlusion cases we tested, both with and without additional regularization, our best performing models had some form of correlated noise. It remains to be investigated whether this trend is robust across other network architectures, types of occlusion, etc. It also remains to be investigated how adding correlated noise to multiple layers (as opposed to a single layer) affects the classification performance of the network. However, sampling from high-

dimensional correlated distributions can be computationally expensive. One of the main areas of focus in the future will be how to balance computational tractability with the performance benefits of incorporating correlation.

We considered Poisson distributions, as cortical neurons display Poisson-like statistics in their spike arrival times. Samples from a Poisson distribution can also approximate dropout in the case when the rates are low. However, we observed that the activations in the Poisson models are highly variable. The standard deviation of Poisson noise scales with the square root of the activation, so we expect that Poisson noise is a weaker regularizer when the activations are higher. This motivates the need for an activity penalty, in addition to the Poisson noise. Our experiments show that dropout paired with Poisson noise is also a strong regularizer, improving recognition performance on the occluded image sets.

While we used a similar version of the straight-through estimator for the Poisson models, there is a way to form a continuous relaxation of a Poisson distribution using the work in [8], [9]. It is also possible to use the idea of deconvolutions/fractional strided convolutions [1] to understand the effect of correlated noise in input space. We intend to pursue this as part of our future work.

ACKNOWLEDGEMENTS

We would like to thank Victor Reyes Osorio and Brittany Reiche for their feedback on this work.

REFERENCES

- [1] M. D. Zeiler and R. Fergus, "Visualizing and Understanding Convolutional Networks," *ArXiv e-prints*, Nov. 2013.
- [2] D. L. K. Yamins, H. Hong, C. F. Cadieu, E. A. Solomon, D. Seibert, and J. J. DiCarlo, "Performance-optimized hierarchical models predict neural responses in higher visual cortex," *Proceedings of the National Academy of Sciences*, vol. 111, no. 23, pp. 8619–8624, 2014.
- [3] E. Zohary, M. N. Shadlen, and W. T. Newsome, "Correlated neuronal discharge rate and its implications for psychophysical performance," *Nature*, vol. 370, pp. 140–143, Jul 1994.
- [4] X. Wang, A. Shrivastava, and A. Gupta, "A-fast-rcnn: Hard positive generation via adversary for object detection," *CoRR*, vol. abs/1704.03414, 2017.
- [5] N. Srivastava, G. Hinton, A. Krizhevsky, I. Sutskever, and R. Salakhutdinov, "Dropout: A simple way to prevent neural networks from overfitting," *J. Mach. Learn. Res.*, vol. 15, no. 1, pp. 1929–1958, Jan. 2014.
- [6] Y. Bengio, N. Léonard, and A. C. Courville, "Estimating or propagating gradients through stochastic neurons for conditional computation," *CoRR*, vol. abs/1308.3432, 2013.
- [7] D. P. Kingma and M. Welling, "Auto-Encoding Variational Bayes," *ArXiv e-prints*, Dec. 2013.
- [8] C. J. Maddison, A. Mnih, and Y. Whye Teh, "The Concrete Distribution: A Continuous Relaxation of Discrete Random Variables," *ArXiv e-prints*, Nov. 2016.
- [9] E. Jang, S. Gu, and B. Poole, "Categorical Reparameterization with Gumbel-Softmax," *ArXiv e-prints*, Nov. 2016.
- [10] B. Poole, J. Sohl-Dickstein, and S. Ganguli, "Analyzing noise in autoencoders and deep networks," *ArXiv e-prints*, Jun. 2014.
- [11] T. DeVries and G. W. Taylor, "Dataset Augmentation in Feature Space," *ArXiv e-prints*, Feb. 2017.
- [12] H. Zhang, M. Cisse, Y. N. Dauphin, and D. Lopez-Paz, "mixup: Beyond Empirical Risk Minimization," *ArXiv e-prints*, Oct. 2017.
- [13] M. A. Smith and A. Kohn, "Spatial and temporal scales of neuronal correlation in primary visual cortex," *Journal of Neuroscience*, vol. 28, no. 48, pp. 12 591–12 603, 2008.
- [14] J. T. Springenberg, A. Dosovitskiy, T. Brox, and M. A. Riedmiller, "Striving for simplicity: The all convolutional net," *CoRR*, vol. abs/1412.6806, 2014.
- [15] M. Abadi, A. Agarwal, P. Barham, E. Brevdo, Z. Chen, C. Citro, G. S. Corrado, A. Davis, J. Dean, M. Devin, S. Ghemawat, I. J. Goodfellow, A. Harp, G. Irving, M. Isard, Y. Jia, R. Józefowicz, L. Kaiser, M. Kudlur, J. Levenberg, D. Mané, R. Monga, S. Moore, D. G. Murray, C. Olah, M. Schuster, J. Shlens, B. Steiner, I. Sutskever, K. Talwar, P. A. Tucker, V. Vanhoucke, V. Vasudevan, F. B. Viégas, O. Vinyals, P. Warden, M. Wattenberg, M. Wicke, Y. Yu, and X. Zheng, "Tensorflow: Large-scale machine learning on heterogeneous distributed systems," *CoRR*, vol. abs/1603.04467, 2016.